Brain Susceptibility Weighted Imaging Signal Changes in Acute Hemorrhagic Anemia: An Experimental Study Using a Rabbit Model

Authors' Contribution:
Study Design A
Data Collection B
Statistical Analysis C
Data Interpretation D
Manuscript Preparation E
Literature Search F
Funds Collection G

AE 1 Jun Xia*
AE 2 Ni Xie*
CD 1 Yuning Feng
CD 1 Anyu Yin
BD 1 Pinni Liu
BC 3 Ruming Zhou
BC 1 Fan Lin
BD 4 Guozhao Teng
BF 1 Yi Lei

1 Department of Radiology, Second People's Hospital of Shenzhen City, First Affiliated Hospital of Shenzhen University, Shenzhen, Guangdong province, China
2 Biobank, Second People's Hospital of Shenzhen City, First Affiliated Hospital of Shenzhen University, Shenzhen, Guangdong province, China
3 Department of Interventional Radiology, Second People's Hospital of Shenzhen City, First Affiliated Hospital of Shenzhen University, Shenzhen, Guangdong province, China
4 Medical Record and Statistics Room, Second People's Hospital of Shenzhen City. First Affiliated Hospital of Shenzhen University, Shenzhen, Guangdong province, China

* The two authors are listed as co-first authors with equal contribution to the paper

Corresponding Author: Yi Lei, e-mail: leiyisz2011@163.com, shzhleiyi@163.com

Background: The aim of this study was to investigate susceptibility-weighted imaging (SWI) signal changes in different brain regions in a rabbit model of acute hemorrhagic anemia.

Material/Methods: Ten New Zealand white rabbits were used for construction of the model of acute hemorrhagic anemia. Signal intensities of SWI images of the bilateral frontal cortex, frontal white matter, temporal lobe, and thalamic nuclei were measured. In addition, the cerebral gray-white contrast and venous structures of the SWI images were evaluated by an experienced physician.

Results: Repeated bloodletting was associated with significant reductions in red blood cell count, hemoglobin concentration, hematocrit, pH, and $PaCO_2$, and elevations of blood lactate and PaO_2. In normal status, the SWI signal intensity was significantly higher in the frontal cortex than in the frontal white matter (63.10±22.82 *vs.* 52.50±20.29; P<0.05). Repeated bloodletting (5 occasions) caused significant (P<0.05) decreases in the SWI signals of the frontal cortex (from 63.10±22.82 to 37.70±4.32), temporal lobe (from 52.50±20.29 to 42.60±5.54), and thalamus (from 60.40±20.29 to 39.40±3.47), but was without effect in the frontal white matter. The cerebral white-gray contrast and venous structures were clearer after bloodletting than before bloodletting.

Conclusions: The effect of hemorrhage on the brain is reflected by SWI signal changes in the cerebral cortex and gray matter nuclei.

MeSH Keywords: Anemia • Cholangiopancreatography, Magnetic Resonance • Hemoglobin, Sickle

Full-text PDF: http://www.medscimonit.com/abstract/index/idArt/890641

📄 2949   ▦ —   📊 5   📑 27

Background

A number of clinical conditions cause acute hemorrhagic anemia, including massive gastrointestinal tract hemorrhage (caused by traumatic surgery, trauma, rupture of gastroesophageal varices, and duodenal and gastric ulcer), pulmonary or bronchial hemoptysis, the sudden bleeding resulting from tumor erosion into the blood vessel wall, and hemostatic defect-related diseases (such as hemophilia, Von Willebrand's disease, and platelet dysfunction) [1–3]. Each of these diseases can decrease blood flow and oxygen supply to the brain, and affect the physiological function of the brain, which often manifests as a wide variety of neurological symptoms, including dizziness, tinnitus, and even stroke and paralysis, and high disability and fatality rates, especially for children. In addition, anemia concurrent with brain trauma and a ruptured aneurysm also easily induces delayed cerebral infarction, thereby affecting treatment effect. Therefore, the detection of changes in brain function in patients with acute hemorrhagic anemia is helpful in preventing neurological complications and evaluating therapeutic effect.

However, the clinical changes of the nervous system in patients with anemia have not received much research attention. One important reason is that the current means can only indirectly detect changes in the brain function following anemia and lag behind the real condition of the brain function. Some methods, such as transcranial Doppler ultrasound, can detect the changes in cerebral blood flow velocity resulting from compensatory response of deficient oxygen delivery in anemia, including the increase in the state of anemia and returning to normal level when anemia is improved, but cannot reflect the actual situation of the oxygen supply and metabolism in the brain or organic brain changes such as stroke [4]. The other means, such as conventional computed tomography (CT) and magnetic resonance imaging (MRI), can detect early cerebral infarction and thus facilitate early treatment, but cannot monitor the physiological changes in the brain from the occurrence of anemia [5]. A non-invasive method, near-infrared spectroscopy (NIRS), is able to measure total levels of blood oxygen in the brain [6–8], but is unable to provide fine details concerning the alterations in different cerebral tissues.

Susceptibility-weighted imaging (SWI) is a newly developed, contrast-enhanced MRI technique that has been used widely in the clinical diagnosis and research of many nervous system diseases, including cerebral hemorrhage and brain tumors [9–12]. SWI is known as high-resolution blood oxygenation level-dependent (BOLD) venographic imaging [13], and can reflect oxygen metabolism-related blood protein concentrations. This technology can produce clear images of cerebral venules, and may be used to detect strokes and microbleeds [11,14–16]. SWI is potentially a novel, non-invasive method for sensing changes in cerebral oxygen levels and may provide more detailed information on cerebral blood flow in patients with

hemorrhage [17]. However, there is a lack of studies in animal models assessing the utility of SWI for monitoring pathophysiologic changes in the brain following acute hemorrhagic anemia.

In the present study, we have used SWI to detect cerebral changes in an animal model of acute hemorrhagic anemia. We found that the SWI images and signals showed changes following hemorrhage, and the extent of the change in the SWI signal following acute hemorrhagic anemia differed between brain parenchyma and white matter regions. This indicates that the partial pressure of oxygen and carbon dioxide, and the concentration of deoxygenated hemoglobin in cerebral blood, are altered following acute hemorrhagic anemia. Our results suggest that SWI may be used to assess various regions of the brain after acute post-hemorrhagic anemia, and that it provides valuable information concerning the pathophysiologic changes in the brain.

Material and Methods

New Zealand white rabbits

Ten male New Zealand white rabbits (weight, 2.1–2.4 kg; age, 3–4 months) were obtained from the Experimental Animal Center of Guangdong Medical College, Guangzhou, China. The study was approved by the Animal Care and Ethics Committee of the First Affiliated Hospital, Shenzhen University, Guangzhou, China. All rabbits were given free access to food and water.

Construction of a rabbit model of acute hemorrhagic anemia

Construction of the rabbit model of acute hemorrhagic anemia was based on the method used by Morimoto et al. [18]. After a 12-h fast, the rabbits were anesthetized by intramuscular injection of 0.2 ml/kg xylazine hydrochloride (Su-Mian-Xin, Veterinary Institute, Academy of Military Medicine Science, Changchun, China). Once the respiratory rate had stabilized at 12–18 breaths/min, the skin of the groin was incised along the groin fold. A catheter was then inserted into the femoral artery, for bloodletting and blood sampling. The blood samples obtained were used for whole blood tests and blood gas analysis (for determination of $PaCO_2$, $PaCO_2$, lactic acid, and pH); in addition, the mean arterial pressure (MAP) was measured. An additional catheter was inserted through the femoral vein to the atrium, for infusion of fluid and assessment of red blood cell count (RBC), hemoglobin concentration (HGB), hematocrit (HCT%), and central venous pressure (CVP).

Blood sampling

Before the first MRI scan was performed, blood samples were drawn for blood gas analysis and whole blood tests. After the first MRI scan had been carried out, a 40-mL blood sample

was drawn through the arterial catheter. To compensate for the effects of simple blood volume loss, the same volume of a 6% hydroxyethyl starch in 0.9% sodium chloride solution was injected through the femoral vein catheter. Following this, a blood sample was drawn again for blood gas analysis and whole blood tests, and the head of the rabbit was re-scanned by MRI. The bloodletting, fluid infusion, and scanning processes were repeated continuously 5 times before the animal recovered from anesthesia; on the fifth occasion, the bloodletting volume and fluid infusion volume were both 50 mL.

MRI scanning

The rabbits were anesthetized, fixed to a special board in the supine position, and scanned by a Siemens Magnetom Avanto 1.5T MRI Scanner (Siemens), using a body coil (excitation) and wrap-around surface coil (reception). T2 dual-echo fast spin-echo with fat-suppression (FSE-T2WI/PD) and SWI 3D sequences were used. The scan extended downward from a plane passing through the superior orbital margin to the medulla oblongata of the rabbit.

FSE-T2WI/PD acquisition was conducted using the following parameters: repetition time (TR)=2800 ms; echo time (TE)=33/78 ms; field of view (FOV)=12×12 cm; matrix size =256×256; and acquisition time =3.09 min. SWI acquisition was performed with a 3D gradient echo sequence, as follows: TR=49 ms; TE=40 ms; flip angle (FA)=15°; FOV=15×15 cm; bandwidth =80 KHz; and IPAT factor =2.

SWI image processing

Additional processing was carried out on the phase-corrected SWI sequences. The third ventricle and the olfactory bulb parallel to the corpus callosum were measured. The bilateral frontal cortex, frontal white matter, temporal lobe, and thalamus were selected manually as regions of interest (ROI). The signal intensity in each of these regions (area fixed at 0.08±0.01 cm^2) was measured, and the average was calculated. The ROI was positioned so as to avoid blood vessels and the skull.

Histology

The rabbits were sacrificed immediately after the fifth MRI scan. The skin was incised and the skull opened. Brain and cerebellum were harvested, immediately fixed in 4% formalin, and embedded in paraffin. Sliced sections (3–5 μm) were stained with hematoxylin and eosin (HE) and examined under an Olympus BX41 microscope.

Statistical analysis

All measurement data are expressed as the mean ± standard deviation. Data analysis was performed using SPSS 21.0 software (IBM). The difference between the 2 groups was analyzed using Students t-test. For all analyses, a value of $P<0.05$ was considered to indicate statistical significance. In addition, a physician with five years of experience of MRI interpretation was invited to evaluate the cerebral white-gray contrast and vein structure of the SWI minimum intensity projection (MIP) images, without knowledge of the sequence in which the images were acquired.

Results

Blood test results

Comparisons of the blood test results before and after bloodletting are shown in Figure 1. There was an approximate halving of the RBC, HGB and HCT% values after the first bloodletting, with further progressive decreases in the values of these parameters following each of the 4 subsequent bloodletting procedures (Figure 1A). The RBC, HGB, and HCT% values after the fifth bloodletting (4.72±0.43×10^{12}/L, 98.20±10.22 g/L and 32.54±3.88%, respectively) were significantly lower than the corresponding control (pre-bleed) values (0.27±0.11×10^{12}/L, 6.01±2.31 g/L and 1.97±1.02%, respectively). The bloodletting procedures were associated with substantial increases in lactic acid concentration as well as a small, but statistically significant, change in blood pH (Figure 1B). After the fifth bloodletting, the lactic acid concentration rose to 14.47±6.30 compared to 3.60±2.48 at pre-bleed. The pH value was decreased from 7.4±0.06 of pre-bleed to 7.25±0.01. PaO$_2$ increased and PaCO$_2$ decreased progressively with each bloodletting procedure (Figure 1C), such that following the fifth bloodletting, PaO$_2$ was significantly elevated (150.40±9.78 vs. 80.53±19.24 mmHg) and PaCO$_2$ was significantly reduced (22.00±7.35 vs. 42.65±4.13 mmHg) compared with the corresponding pre-bleed values. Bloodletting was not associated with any changes in CVP or MAP (Figure 1D). These results suggest the successful construction of acute hemorrhagic anemia in experimental rabbits.

SWI signals and images

The SWI signals of rabbit brains were acquired before and after bloodletting. Figure 2 shows representative SWI and corresponding T2-weighted images of the brain of a rabbit, obtained at the superior aspect of the olfactory bulb, the border of the olfactory bulb, the thalamus, and the cerebellum; also evident are examples of the ROIs chosen for analyses of the SWI images (see Materials and Methods). The mean SWI signal intensities (arbitrary units) of the frontal cortex, frontal white matter, temporal lobe, and thalamus, before and after bloodletting, are presented in Figure 3. The control (pre-bleed) SWI signal intensity of the frontal white matter was significantly lower than that of the frontal cortex (52.50±20.29 vs.
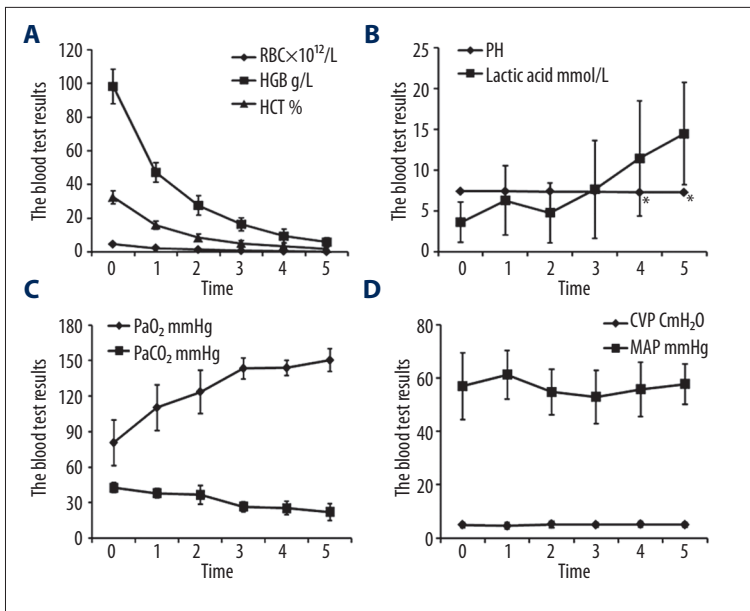
Figure 1. The effects of repeated bloodletting on the results of whole blood tests, blood gas analyses, mean arterial pressure, and central venous pressure. (**A**) Repeated bloodletting was associated with progressive reductions in red blood cell count (RBC), hemoglobin concentration (HGB), and hematocrit (HCT%). (**B**) Repeated blood loss resulted in an increase in blood lactic acid concentration and a decrease in pH. (**C**) Bloodletting resulted in a progressive increase in the arterial partial pressure of oxygen (PaO_2), and a progressive decrease in the arterial partial pressure of carbon dioxide ($PaCO_2$). (**D**) Blood loss was not associated with changes in mean arterial pressure (MAP) or central venous pressure (CVP). Data are presented as mean ± standard deviation, * P<0.05.
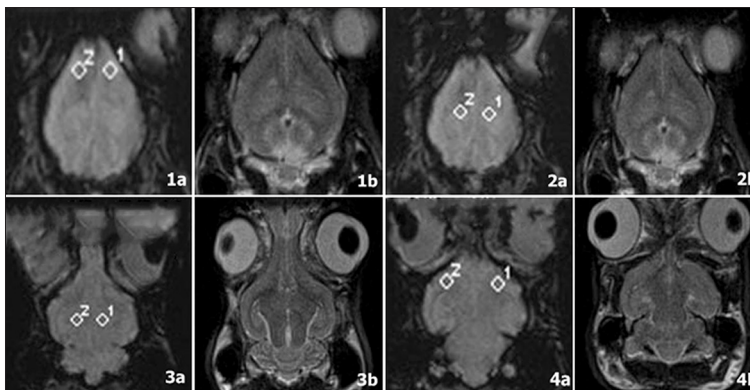

Figure 2. Representative SWI (panels **1a–4a**) and corresponding T2-weighted (**1b–4b**) images of the brain of a rabbit, obtained at the superior aspect of the olfactory bulb (**1a, 1b**), the border of the olfactory bulb (**2a, 2b**), the thalamus (**3a, 3b**), and the cerebellum (**4a, 4b**). In the SWI images, ROIs are indicated by numbers as follows: **1a** (squares 1 and 2): frontal lobe cortex (left and right sides); **2a** (squares 1 and 2): frontal lobe brain parenchyma (left and right sides); **3a** (squares 1 and 2): thalamus (left and right sides); and **4a** (squares 1 and 2): temporal lobe cortex (left and right sides). For all images, the anterior aspect of the brain is toward the top of the image, and the left side of the brain is toward the right, as indicated in panel **1a**.
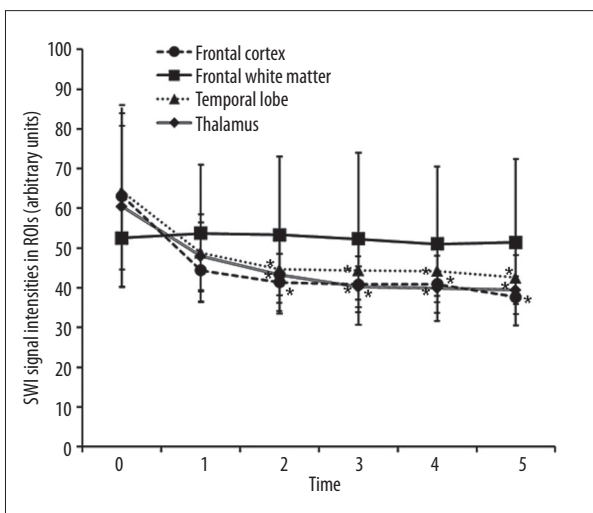

Figure 3. The effects of repeated bloodletting on the SWI signal intensities of selected regions of the brain. Repeated bloodletting was associated with reductions in the mean SWI signal intensities of the frontal cortex, temporal lobe, and thalamus, but not of the frontal white matter. Data are shown as means ± standard deviations. Compared with the control (pre-bleed) value, significant (P<0.05) decreases in SWI signal intensity were observed for the frontal cortex, temporal lobe, and thalamus following the second, third, fourth, and fifth bloodlettings; the values after the first bloodletting were not significantly different from the control (pre-bleed) values. For the frontal white matter, none of the values after bloodletting were significantly different from the control (pre-bleed) value.
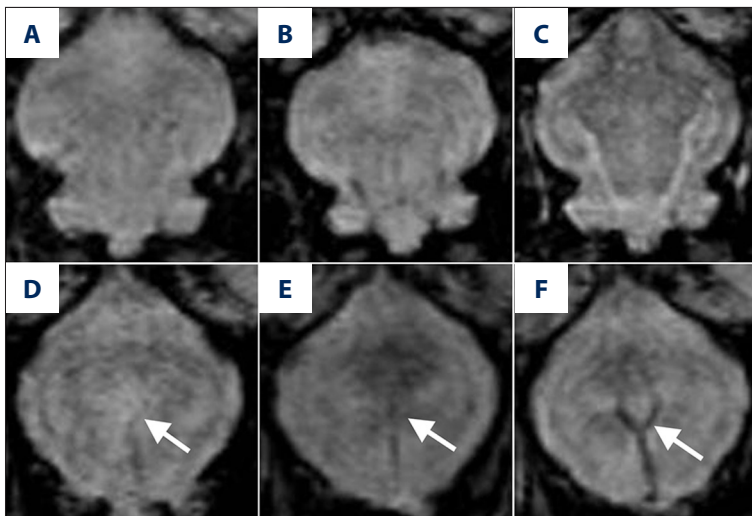
Figure 4. Images of the thalamus and cerebral veins obtained by magnetically sensitive scanning. Images of the thalamus are shown before bloodletting (**A**), after the first bloodletting (**B**), and after the fifth bloodletting (**C**). The cerebral white-gray contrast of the gray matter becomes clearer with repeated blood loss. Images of the central veins are shown before bloodletting (**D**), after the first bloodletting (**E**), and after the fifth bloodletting (**F**). The vein structure (arrows) also becomes clearer with repeated blood loss.
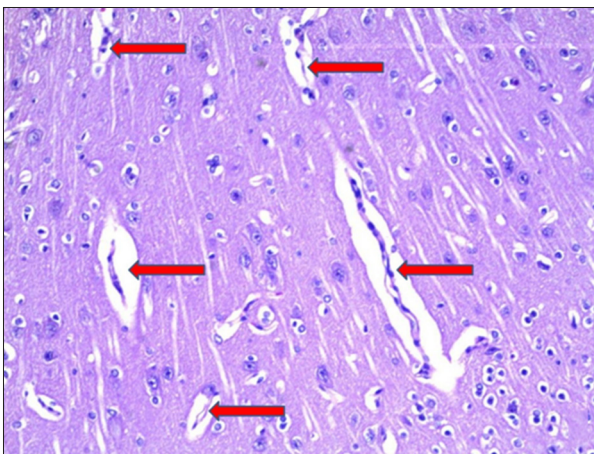

Figure 5. Histological section of the brain after bloodletting (HE, ×100). Spaces (arrows) had formed around the blood vessels and cells, indicative of the development of cerebral edema.

63.10 ± 22.82; $P < 0.05$). Bloodletting was not associated with any significant changes in the SWI signal of the frontal white matter. In contrast, there were significant ($P < 0.05$) decreases in the SWI signals of the frontal cortex, temporal lobe, and thalamus after the second, third, fourth, and fifth bloodletting procedures, compared with the corresponding control (pre-bleed) values. Following the fifth bloodletting, the SWI signal intensities of the frontal cortex, temporal lobe, and thalamus were 37.70 ± 4.32, 42.60 ± 5.54, and 39.40 ± 3.47, compared with corresponding control (pre-bleed) values of 63.10 ± 22.82, 52.50 ± 20.29, and 60.40 ± 20.29, respectively ($P < 0.05$).

The value of the ROI only reflects the signal intensity of a localized region of the brain, and may be influenced by the volume effect. Therefore, we also evaluated the overall cerebral white-gray contrast and vein structure by inviting a physician with 5 years of experience to examine the SWI MIP images

recorded before and after bloodletting (Figure 4). The physician was blinded to the sequence in which the images were taken. The interpretation of the physician was that, compared with the control (pre-bleed) images, the contrast between the cerebral gray and white matter was higher after bloodletting, particularly after the fourth and fifth bloodletting procedures, and that venous structure was more abundant and clearer after bloodletting.

Histology

Histological sections of brain tissues after bloodletting revealed that degeneration and necrosis of neurons and glial cells were not evident (Figure 5). However, spaces had formed around the blood vessels and cells, consistent with the occurrence of cerebral edema.

Discussion

Recent studies have demonstrated that the cerebral venous contrast of SWI images and the SWI signal intensity of brain tissues change when certain drugs (such as narcotics, caffeine, and contrast agents) are applied or certain pathophysiologic conditions are present [19,20]. In the present study, SWI was used to investigate the association between the SWI signal intensities of various regions of the rabbit brain and the partial pressures of blood oxygen and carbon dioxide in these regions, after acute hemorrhagic anemia.

The rabbits in our study were anesthetized during MRI scanning. To remove the possible influence of the anesthetic on the partial pressures of oxygen and carbon dioxide in the blood, and thereby on the BOLD signal intensity, we compared the SWI signal intensities of different brain regions of the anesthetized rabbits before and after bloodletting.

Our results showed that following the hemorrhage, the RBC count, hemoglobin, and hematocrit of the rabbits decreased, indicative of a state of hemorrhagic shock. After bloodletting, the rabbits were injected with hydroxyethyl starch in sodium chloride solution to maintain blood volume and venous return in the short term and hence improve organ perfusion, resulting in little or no change in the CVP and MAP values of the rabbits. This supplement of fluid is often used as emergent treatment of patients in hemorrhagic or extensive burn situations. However, although the hydroxyethyl starch/sodium chloride solution was able to increase blood volume, it did not replenish the red blood cells that carry oxygen, and hence it could not correct the problem of inadequate tissue oxygenation. As a result, the PaO_2 increased significantly and the $PaCO_2$ decreased significantly. The blood lactate levels initially increased, then decreased to some extent, and finally increased again. A possible explanation for this is that at the early stage of blood loss, a rapid decrease in blood volume led to tissue hypoperfusion and an increase in anaerobic metabolism; subsequently, the injection of hydroxyethyl starch/sodium chloride solution caused an increase in blood volume that partially replenished the blood oxygen, thereby reducing lactic acid levels; and finally, as more hydroxyethyl starch/sodium chloride solution was injected into the rabbits, the acidic substances deposited in the tissues were able to enter the bloodstream and cause an elevation of the lactic acid level.

The BOLD signal is closely related to intravenous oxygen concentration and can indirectly reflect changes in cerebral blood flow (CBF), thereby allowing the monitoring of oxygen saturation. SWI calculates the oxygen saturation based on the differences in the magnetic sensitivities of oxyhemoglobin and deoxyhemoglobin [21]. The SWI images of venous structures depend on the T2* time, which may be shortened by deoxyhemoglobin-induced non-uniformity of the magnetic field, and phase differences between the surrounding tissue and blood vessels [22]; therefore, changes in CBF can also cause changes in the SWI signals [21]. The R2* parameter of BOLD may be affected by blood volume, the red blood cell volume ratio, oxygen consumption, and small arteries [23], as well as by other factors such as subject age [24]. Since SWI is an imaging technique with full flow compensation, it has a higher sensitivity than BOLD MRI when the magnetic field is uneven [25], and therefore can minimize the interference of small arteries in the measurement and can accurately detect deoxygenated hemoglobin.

The results presented here demonstrate that after repeated bloodletting in rabbits, the SWI signal intensities of gray matter structures in the bilateral frontal cortex, temporal lobe, and thalamus were significantly decreased. However, the SWI signal intensity of the frontal white matter was not significantly affected by bloodletting. The reductions in the SWI signal intensities of the bilateral frontal cortex, temporal lobe, and thalamus after bloodletting may have been the result of decompensation induced by the repeated loss of blood. Bloodletting may have resulted in a fall in blood pressure, an elevation of heart rate, and hyperventilation, further increasing the emission of carbon dioxide and thus decreasing its partial pressure, as was evident from our observations. The resulting hypocapnia may have led to cerebral artery contractions and reductions in CBF. To meet the oxygen needs of the brain, the proportion of oxygen extracted from the blood must increase, thereby decreasing cerebral venous oxygen, elevating levels of intravenous deoxyhemoglobin, and reducing the SWI signal intensity.

Previous studies have revealed that the overall metabolic rate, the number of capillaries in gray matter, and the flow rate of the cerebral cortex are 4 times that of the white matter [26]. Our study also demonstrated that before bloodletting the SWI signal intensity of the frontal cortex of rabbits was significantly higher than that of the frontal white matter, suggesting higher perfusion and more perfusion-induced oxyhemoglobin in the gray matter than in the white matter. Furthermore, the results presented here imply that the gray matter was more sensitive to changes in PaO_2 and $PaCO_2$ caused by acute hemorrhage, consistent with a previous report using arterial spin-labeling MR imaging [27]. In our study, blood loss led to a decrease in the SWI signal intensities of the gray matter structures of the cortex and thalamus, but little or no change in the white matter structures, suggesting that in the hypocapnic state associated with acute hemorrhage, the reductions in cerebral perfusion in the cortex and thalamic nuclei were greater than that in the white matter. In contrast to our findings, Rostrup et al. [27] reported that in conscious volunteers scanned using functional MRI, elevations in blood carbonic acid content were associated with increases in the BOLD signal intensity of only the cortical gray matter, with no rise detected in the gray matter nuclei and white matter. A possible explanation for this discrepancy is that the use of anesthetics in our study may have inhibited gray matter structures; in addition, SWI is more sensitive and accurate at measuring alterations in BOLD signal intensities, allowing detection of changes in the gray matter nuclei that may not have been detectable in the Rostrup et al. study. Moreover, we evaluated the cerebral white-gray contrast of the SWI images. The gray matter of the brain contains more veins than the white matter, which may explain our observation that the SWI signal of the white matter was not significantly decreased. During the hemorrhage, cerebral venous structures became clearer, and the cerebral white-gray contrast was markedly improved.

Conclusions

This study has revealed that SWI is an effective tool for detecting PaO_2- and $PaCO_2$-induced changes in the cerebral

oxygenation of different brain regions after acute hemorrhagic anemia. Therefore, SWI may be a useful technique for monitoring the pathophysiological changes and related complications associated with acute anemia.

References:

1. Raphaeli T, Menon R: Current treatment of lower gastrointestinal hemorrhage. Clin Colon Rectal Surg, 2012; 25: 219–27

2. Jin S, Fu Q, Wuyun G, Wuyun T: Management of post-hepatectomy complications. World J Gastroenterol, 2013; 19: 7983–91

3. Hurt K, Bilton D: Haemoptysis: diagnosis and treatment. Acute Med, 2012; 11: 39–45

4. Purkayastha S, Sorond F: Transcranial Doppler ultrasound: technique and application. Semin Neurol, 2012; 32: 411–20

5. Allmendinger AM, Tang ER, Lui YW, Spektor V: Imaging of stroke: Part 1, Perfusion CT – overview of imaging technique, interpretation pearls, and common pitfalls. Am J Roentgenol, 2012; 198: 52–62

6. Yamazaki K, Suzuki K, Itoh H et al: Cerebral oxygen saturation evaluated by near-infrared time-resolved spectroscopy (TRS) in pregnant women during caesarean section – a promising new method of maternal monitoring. Clin Physiol Funct Imaging, 2013; 33: 109–16

7. Navarro LH, Lima RM, Khan M et al: Continuous measurement of cerebral oxygen saturation (rSO(2)) for assessment of cardiovascular status during hemorrhagic shock in a swine model. J Trauma Acute Care Surg, 2012; 73: S140–46

8. Murkin JM, Arango M: Near-infrared spectroscopy as an index of brain and tissue oxygenation. Br J Anaesth, 2009; 103(Suppl.1): i3–13

9. Huang P, Chen CH, Lin WC et al: Clinical applications of susceptibility weighted imaging in patients with major stroke. J Neurol, 2012; 259: 1426–32

10. Niwa T, de Vries LS, Benders MJ et al: Punctate white matter lesions in infants: new insights using susceptibility-weighted imaging. Neuroradiology, 2011; 53: 669–79

11. Lee YJ, Shon YM, Yoo WJ et al: Diminished Visibility of Cerebral Venous Vasculature in Subclinical Status Epilepticus by Susceptibility-Weighted Imaging: A Case Report. Clin Neuroradiol, 2014; 24(1): 69–72

12. Roelcke U, Boxheimer L, Fathi AR et al: Cortical hemosiderin is associated with seizures in patients with newly diagnosed malignant brain tumors. J Neurooncol, 2013; 115: 463–68

13. Boeckh-Behrens T, Lutz J, Lummel N et al: Susceptibility-weighted angiography (SWAN) of cerebral veins and arteries compared to TOF-MRA. Eur J Radiol, 2012; 81: 1238–45

14. Santhosh K, Kesavadas C, Thomas B et al: Susceptibility weighted imaging: a new tool in magnetic resonance imaging of stroke. Clin Radiol, 2009; 64: 74–83

15. Goos JD, van der Flier WM, Knol DL et al: Clinical relevance of improved microbleed detection by susceptibility-weighted magnetic resonance imaging. Stroke, 2011; 42: 1894–900

16. Cheng AL, Batool S, McCreary CR et al: Susceptibility-weighted imaging is more reliable than T2*-weighted gradient-recalled echo MRI for detecting microbleeds. Stroke, 2013; 44: 2782–86

17. Li M, Hu J, Miao Y et al: *In vivo* measurement of oxygenation changes after stroke using susceptibility weighted imaging filtered phase data. PLoS One, 2013; 8: e63013

18. Morimoto Y, Mathru M, Martinez-Tica JF, Zornow MH: Effects of profound anemia on brain tissue oxygen tension, carbon dioxide tension, and pH in rabbits. J Neurosurg Anesthesiol, 2001; 13: 33–39

19. Rauscher A, Sedlacik J, Barth M et al: Nonnvasive assessment of vascular architecture and function during modulated blood oxygenation using susceptibility weighted magnetic resonance imaging. Magn Reson Med, 2005; 54: 87–95

20. Sedlacik J, Helm K, Rauscher A et al: Investigations on the effect of caffeine on cerebral venous vessel contrast by using susceptibility-weighted imaging (SWI) at 1.5, 3 and 7 T. Neuroimage, 2008; 40: 11–18

21. Shen Y, Kou Z, Kreipke CW et al: *In vivo* measurement of tissue damage, oxygen saturation changes and blood flow changes after experimental traumatic brain injury in rats using susceptibility weighted imaging. Magn Reson Imaging, 2007; 25: 219–27

22. Haacke EM, Xu Y, Cheng YC, Reichenbach JR: Susceptibility weighted imaging (SWI). Magn Reson Med, 2004; 52: 612–18

23. Fan Z, Elzibak A, Boylan C, Noseworthy MD: Blood oxygen level-dependent magnetic resonance imaging of the human liver: preliminary results. J Comput Assist Tomogr, 2010; 34: 523–31

24. Haacke EM, Miao Y, Liu M et al: Correlation of putative iron content as represented by changes in R2* and phase with age in deep gray matter of healthy adults. J Magn Reson Imaging, 2010; 32: 561–76

25. Guyton AC, Hall JE. Cerebral blood flown cerebrospinal fluid and brain metabolism. Philadelphia: Elsevier Saunders; 2006

26. Floyd TF, Clark JM, Gelfand R et al: Independent cerebral vasoconstrictive effects of hyperoxia and accompanying arterial hypocapnia at 1 ATA. J Appl Physiol (1985), 2003; 95: 2453–61

27. Rostrup E, Larsson HB, Toft PB et al: Functional MRI of CO2 induced increase in cerebral perfusion. NMR Biomed, 1994; 7: 29–34

Conflict of interests

All authors declare that they have no conflict of interest.